Vol.4 No.4 Oct 2021

Multimedia Research

Received 24 August, Revised 20 September, Accepted 10 October

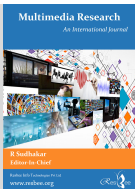

Hybrid Flower Pollination Algorithm and Binary Particle Swarm Optimization Algorithm for Osteosarcoma Detection

Manaswi Sachin Kulkarni

Tech Mahindra Americas Inc, Dallas, TX, USA

Abstract: Generally, Osteosarcoma is represented as malignant bone sarcoma which is typified by an extensive genomic disruption and a proclivity for metastatic extend. Due to the early recognition, Osteosarcoma raises the human beings' survival rate. During the early phase, several Osteosarcoma recognition approaches are developed in order to recognize the Osteosarcoma, however, evaluating the slides in the microscope to identify the tumor necrosis degree and tumor outcome is an important challenge in the medical segment. Therefore, an effectual recognition approach is modeled by exploiting the adopted Hybrid Flower Pollination algorithm with the Binary Particle Swarm Optimization algorithm based Generative Adversarial Network (FPO-BPSO based GAN) to detect the osteosarcoma during the initial phase. Moreover, the adopted FPO-BPSO is modeled using the combination of FPA and BPSO, correspondingly. As a result, the classification of the important tumor, non-tumor, as well as necrotic tumor is performed using GAN by exploiting the histology image slides. GAN is exploited to carry out the osteosarcoma recognition based on features extracted from the image via the cell segmentation process. The GAN training process is performed by exploiting the adopted Hybrid FPO-BPSO approach. Nevertheless, the adopted FPO-BPSO attained superior performance by exploiting the measures, like accuracy, sensitivity, and specificity.

Keywords: Cell Segmentation, GAN, Image, Microscope, Osteosarcoma, Tumor.

Nomenclature

Abbreviations	Descriptions
OS	Osteosarcoma
WHO	World Health Organization
TEM	Transmission Electron Microscopy
NN	Neural Networks
G-3D Au	Graphene-three Dimensional Nanostructure Gold Nanocomposites
BSA	Bull Serum Albumin
SEM	Scanning Electron Microscopy
DTNB	Dithiobis 2-Nitrobenzoic Acid
AuNCs	Gold Nanoclusters
SVM	Support Vector Machine
SERS	Surface-Enhanced Raman scattering
SLBP	Significant Local Binary Pattern
H&E	Hematoxylin and Eosin
ML	Machine Learning
ALP	Alkaline Phosphatase
C-path	Computational pathologist

1. Introduction

Generally, OS is considered one of the most important bone malignant tumors, warns life as well as adolescent health dangerously. Even though, the chemotherapy of neoadjuvant raises the five-year survival rate of osteosarcoma patients, the tumor cells metastasis is still a motivation for patient's death with osteosarcoma [1]. When patients with lung metastases are 36%5, studies have shown that the osteosarcoma patient's survival rate without lung metastases is about 74%. Hence, tumor cell detection earlier is important to improve the osteosarcoma survival rate. Conventional, techniques such as computerized tomography, magnetic resonance imaging, fluorescent microscopy, and flow cytometry were used for the detection of cancer cells, nevertheless, the drawbacks, like time consumption as well as high

https://doi.org/10.46253/j.mr.v4i4.a1

cost, in either investigational procedure or instrumentation, highly restrict their widespread application. Hence, it is significant to expand quick, effortless techniques for early cancer cell detection [2].
Generally, the Osteosarcoma represents a bone malignant neoplasm. It is also considered the basic bone malignant tumor that occurs in children as well as adults and also it is considered the 3rd general malignancy in both adolescents and children. The WHO is sub-classified into osteosarcoma histologic manifestation to surface and central tumors as well as identifies a number of subcategories within every group. In the proximal humerus metaphysic, Osteosarcoma regularly originates proximal tibia and distal femur. The alternatives are a heterogeneous group of osteosarcomas with a range of diverse imaging as well as behavioral features [3].

In recent times, by exploiting the microscope, manually pathologists assess the slides to examine the degree of the tumor as well as tumor necrosis. In patients, the treatment response degree of cancer is estimated by exploiting the H&E stained images by pathologists to discover necrosis proportion that is time utilizing procedure as well as it is flat to imprecision and observer bias. Recently decades, machine learning approaches, such as NN are generally exploited to carry out image segmentation and classification. Nevertheless, numerous tumor researchers' focal points in recognizing the superset of appropriate features. The current research exhibited that lung cancer with nonsmall cells isolated approximately 9000 features from images which comprise factors extracted from color, texture, identification, granularity, density, etc. Nevertheless, the machine learning techniques are extensively exploited in the C-path system to extract the morphological features robotically from both tumor cells and neighboring stroma from microarrays of breast cancer tissues. Consequently, from the stromal tissue, the features are recognized which are exploited and attain superior prediction of survival rate of the patient. Logistic regression, Random forest, and SVM are exploited to classify osteosarcoma by exploiting serum samples' metabolomic profiles [4]. The ML techniques, such as the Bayesian classifier and SVM are efficient, however, they require high training data volume so the training stage consequence a time utilize task [13] [14].

The major objective of this work is to recognize osteosarcoma by exploiting the adopted Hybrid FPO-BPSO approach. The adopted model carries out the recognition procedure by including the stages such as pre-processing, segmentation of cells, feature extraction as well as detection of osteosarcoma. At first, the input image is subjected to preprocessing stage wherein noise as well as the exterior artifacts is evaded from the image. Nevertheless, pre-processed image is subjected to the cell segmentation phase; exploiting Renyi entropy-based hybrid integration technique the segmentation process is performed. Subsequent to image segmentation, the features related to the image are extracted high efficiently. Following, the feature extraction completion, osteosarcoma detection is performed by exploiting the GAN that is trained by exploiting the adopted Hybrid FPO-BPSO approach.

2. Literature Review

In 2019, Hao-Hua Deng wt al [1], worked on the AuNCs and was paying attention to a great deal of concentration as signal transducers in photoluminescence biological/chemical sensors. In this, Fe3+ as a quencher, bovine serum albumin/3-mercaptopropionic acid co-enhanced AuNCs as a fluorescence probe, as well as pyrophosphate as an ALP substrate as well as Fe3+ chelator to model a new biosensor for ALP recognition, attaining a recognition linear range of 0.8–16 U/L as well as a recognition limit of 0.78 U/L was employed.

In 2018, Zhao-Yang Wu et al [2], developed a new electrochemical cytosensor to detect the human osteosarcoma B cells on the basis of G-3D Au by exploiting the simplistic as well as speedy one-step electrochemical co-reduction approach. Characterization by SEM and TEM shows that gold nanoparticles in scale concerning the 5-80 nm were deposited.

In 2017, F. Lamonaca et al [3], worked on the characterization, using measurement approaches characteristically exploited for polymeric as well as ceramics materials, of human bone samples affected by two aggressive tumors: sclerotic and osteolitic osteosarcoma. Aforesaid two general types of osteosarcoma frequently affect children and young teenagers. To differentiate between diseased as well as healthy bone tissue, the Hydroxyapatite/ Collagen ratio and the Hydroxyapatite composition were estimated. The outcomes permit two classifications to be performed on the human bone samples analysis.

In 2016, Ji Yue et al [4], worked on the SERS which was extensively exploited in the sensing as well as imaging field. Nevertheless, restricted analysis was recently obtainable on the SERS-based cancer cell targeting approach because of reproducible synthesizing highly sensitive, as well as biocompatible SERS probe challenging. In this paper, new SERS probes were modeled, on the basis of the BSA and, DTNB for in vitro cancer cell recognition.

In 2016, Lavinia Ferrante di Ruffano and Tony Waldron [5], worked on radiographic images that corroborate medullary participation, lack of continuity among cortex as well as external mass, a

radiolucent cleavage plane, and probable radiolucent zones in bony masses. Discrepancy diagnoses taken into consideration comprise myositis ossificans, osteochondroma, fracture callus, and most important malignancies of chondrosarcoma as well as osteosarcoma, and their variety of subcategories. The radiographic, as well as macroscopic analysis of the tumor, was explained and analyzed within paleopathological as well as clinical contexts.

3. Developed Model for the Detection of Osteosarcoma

Generally, Osteosarcoma occurs in the area of fast bone growth such as distal as well as proximal tibia so it is represented as a malignant bone tumor. In the clinical phase, recognizing the osteosarcoma in an accurate manner is considered a challenging task. Hence, an effectual osteosarcoma recognition model is adopted by exploiting the adopted hybrid FPO-BPSO approach. The developed model carries out the recognition procedure by including the stages such as pre-processing, segmentation of cells, feature extraction, and detection of osteosarcoma. In the pre-processing stage, the input image is transmitted wherein the image is pre-processed which is highly effective as well as precise. Subsequently, to the cell segmentation stage pre-processed image is transmitted wherein Renyi entropy-based hybrid integration approach is exploited to segment images. Nevertheless, blackhole fuzzy clustering, as well as the active contour model, is exploited to design the hybrid fusion model. Subsequent to image segmentation, features such as segment-level features statistical features, as well as image-level features, are effectually extracted. At last, by exploiting the GAN, the osteosarcoma is recognized and then the proposed hybrid FPO-BPSO optimization approach is exploited to train GAN. Fig. 1 demonstrates the architectural model of the adopted hybrid FPO-BPSO optimization model.

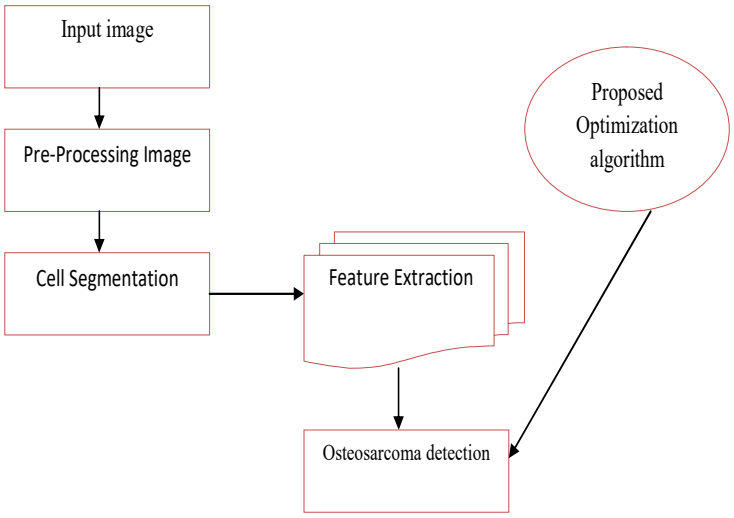

Fig.1. *Architectural model of the developed FPO-BPSO based GAN*

3.1 Input Image Acquisition

To carry out the osteosarcoma recognition, the input image is exploited which is an H&E stained osteosarcoma histology image that is obtained from the dataset [6]. A precise, as well as the highly complete perspective of disease, is provided by the histology image as well as their effect on tissues. By exploiting the histology image osteosarcoma detection is considered a bullion standard in the clinical field. In the image view, the extra structure of these images presents a higher number of information. Assume that the γ as a dataset with j count of histology images G is stated as

$$\gamma = \{G_i\}; 1 \le i \le j \quad (1)$$

wherein, G_i signifies histology image positioned at i^{th} dataset index and j signifies total count of images,. The image G_i is exploited to carry out the osteosarcoma recognition by transmitting the image to pre-processing phase.

3.2 Input Image Pre-processing

In the pre-processing phase, G_i image is subjected to wherein the image is effectually pre-processed by evading the noise from the image. The associative tissue, cytoplasm as well as cell nuclei are effectually

separated by means of an H&E stained histology image. The fat of tissue also named the background is evaded from the input image G_i in the pre-processing stage. The pre-processed image is represented as,

$$\mathrm{I} = \chi(\mathrm{G_i}) \tag{2}$$

Where in, I signifies pre-processed image as well as χ signifies pre-processing. Nevertheless, the pre-processed image I is transmitted to the cell segmentation phase to perform the detection of osteosarcoma.

3.3 Renyi Entropy-based Hybrid Integration for Cell Segmentation

In the cell segmentation phase, the pre-processed outcome I is subjected, wherein the cell segmentation process is examined by exploiting Renyi entropy-based hybrid integration. It is necessary to segment histology images to intrinsically untie individual nuclei or cells. The cell segmentation process is exploited in order to recognize the cell boundaries, cell nuclei as well as histological structure by means of the stained tissue. Moreover, the cell segmentation process is attained by exploiting the newly modeled Renyi entropy-based hybrid fusion approach [7] [8]. Nevertheless, the hybrid integration approach is modeled by combining the active contour model with blackhole fuzzy entropy, correspondingly.

Active contour model: It is worked on basis of internal as well as external forces that pull contour towards image features. Nevertheless, eq. (3) indicates the active contour model. P_{ext} signifies external energy and P_{int} signifies internal energy.

$$\mathrm{D^r} = \mathrm{P} = \int_{\hbar=0}^{1} \mathrm{P_{int}}(\sigma(\hbar)) + \mathrm{P_{ext}}(\sigma(\hbar))\mathrm{d}\hbar \tag{3}$$

Blackhole fuzzy clustering: By realizing the fuzzy clustering, it is exploited to verify the black holes' nature. Moreover, the fuzziness, as well as the probability, is combined with the fuzzy clustering. Nevertheless, by exploiting the Bayesian interference, the clusters of fuzzy clustering are calculated [7]. In addition, the mathematical formulation of blackhole fuzzy clustering is represented as Eq. (4), V signifies clustering center set, W signifies dataset, and Z signifies membership matrix, correspondingly.

$$\mathrm{D^s} = \mathrm{BHE}(\mathrm{W},\mathrm{V},\mathrm{Z}) = \min_{\mathrm{V,Z}} \sum_{0=1}^{\mu_1} \sum_{\mathrm{w}=1}^{\mu_2} \left(\mathrm{z_{ow}} \left\| \mathrm{aa_w} - \mathrm{bb_o} \right\|^2 + \alpha \ln \mathrm{aa_{ow}} + \alpha \ln \left\| \mathrm{aa_w} - \mathrm{bb_o}^2 \right\| \right) \tag{4}$$

The active contour model $\mathrm{D^r}$ indicates the outcome attained, as well as $\mathrm{D^s}$ represents the outcome attained from the blackhole fuzzy clustering. Moreover, the mathematical formulation of the Renyi entropy-based hybrid fusion approach [8] is stated as eq. (5), wherein, $\mathrm{D^r_{u,v}}$ signifies pixel entropy positioned at $\mathrm{D^r}$, and $D^s_{u,v}$ signifies pixel positioned entropy at D^s. For that reason, M is indicated as eq. (6), wherein, δ specifies Renyi entropy, $\mathrm{D^r_{n(u,v)}}$ specifies neighbor of $\mathrm{D^r}$, and $\mathrm{D^s_{n(u,v)}}$ specifies neighbor of $\mathrm{D^s}$, correspondingly. Hence, the outcome attained from the process of cell segmentation is indicated as D, that is fed to the features extraction phase to extract necessary as well as helpful features.

$$\mathrm{D_{u,v}} = \begin{cases} \mathrm{D^r_{u,v}} & ; \text{if } \mathrm{D^r_{u,v}} = \mathrm{D^s_{u,v}} \\ \mathrm{M} & ; \text{otherwise} \end{cases} \tag{5}$$

$$\mathrm{M} = \begin{cases} \mathrm{D^r_{n(u,v)}} & ; \text{if } \mathrm{M_1} < \mathrm{M_2} \\ \mathrm{D^s_{n(u,v)}} & ; \text{otherwise} \end{cases} \tag{6}$$

$$\mathrm{M_1} = \delta\left(\mathrm{D^r_{n(u,v)}}\right) \tag{7}$$

$$\mathrm{M_2} = \delta\left(\mathrm{D^s_{n(u,v)}}\right) \tag{8}$$

3.4 Feature Extraction

The process of feature extraction is exploited to minimize the image dimensionality by choosing the helpful features that facilitate augmenting the accurateness of osteosarcoma recognition. From histology images to extract the features, D output attained from the process of cell segmentation is transmitted as input to the feature extraction step. Moreover, from segmented histology images, the features, such as image-level features, statistical features, as well as segment-level features are extracted.

a) Statistical features: The statistical features, such as variance, mean as well as standard deviation and it is demonstrated as follows:

Mean: For enhanced asymmetry analysis this feature is extracted. Nevertheless, from the segmented histology image the mean feature extracted is represented as Eq. (9), wherein, F signifies the total count of samples, D signifies segmented images, correspondingly.

$$X_1 = \frac{1}{F}\sum_{h=1}^{F} D_h \tag{9}$$

Variance: It indicates the tumor region spread in histology image as well as it is calculated by exploiting the eq. (10).

$$X_2 = \frac{1}{F}\sum_{h=1}^{F} (D_h - X_1)^2 \tag{10}$$

Standard deviation: It is calculated on basis of the variance feature and indicated as,

$$X_3 = \sqrt{\frac{1}{F}\sum_{h=1}^{F} (D_h - X_1)} \tag{11}$$

b) Segment level features: This feature comprises red cell count as well as blue cell count, and nuclear count which is described below:

Red cell count as well as blue cell count: From stained images, foreground, as well as background pixels, are separated. Moreover, X_4 indicates red cell count, when X_5 represents as red cell count correspondingly.

Nuclear count: X_6 indicates density property which is extracted from the segmented.

c) Image level features: This feature comprises SLBP [9] feature extracted from histology image segmented cell.

SLBP: By exploiting the important factors the local texture features of the image are indicated so that SLBP is indicated as eq. (12), wherein, q_y specifies y^{th} pixel grey value, q_e specify the center pixel value, and $x(q_e)$ specify important center pixel factor. The feature vector used to carry out osteosarcoma recognition is indicated as eq. (13), wherein, X states the feature vector with a dimension of $[U \times V]$, and w states the total count of features, correspondingly.

$$X_7 = x(q_e)\sum_{y=1}^{Q} g(q_y, q_e)2^y \tag{12}$$

$$X = \{X_w\}; w \in \{1,2,\ldots,7\} \tag{13}$$

3.5 Osteosarcoma Detection by Exploiting FPO-BPSO on the basis of GAN

Subsequent to extraction, the important as well as the practical features from histology image, osteosarcoma recognition procedure is performed by exploiting the GAN that is trained exploiting adopted optimization approach. Osteosarcoma is a genetic disease that starts in fibrous tissue, bone, muscles, as well as other human body tissues. The tumor develops in bone and affects growth as well as bone movement. In the medical phase, untimely recognition of osteosarcoma presents additional treatment choices. Therefore, it is essential to recognize the osteosarcoma at an earlier phase. The GAN is exploited in order to perform the detection process so that the training process of GAN is attained by the adopted FPO-BPSO model.

3.5.1 Architecture of GAN

Using the adversarial process, a feature vector X is taken by GAN which is input and carries out the detection of osteosarcoma. During the learning process, GAN [10] [11] is more stable therefore it is efficiently exploited to detect osteosarcoma. The GAN operation is on the basis of min-max two-player games which offer an influential manner for estimating the target distribution and producing new samples. GAN comprises two adversarial techniques, the discriminative model R as well as a generative model J. Nevertheless, the generative model is exploited to capture the feature vectors, while the

discriminative approach is exploited to estimate the probability on the basis of the training data. In addition, GAN forms an adversarial game among discriminators as well as generators. Here, input is the feature vector that is exploited by the generator and attempts to produce a count of samples to create a discriminator hoodwink, wherein the discriminator is trying to identify if the sample is attained from the model or image distribution. Assume real data points as X, real data distribution as Y_{data}, a indicates the high dimensional arbitrary variable, J_{dis} represents the generator distribution and K represents an arbitrary variable, correspondingly. The arbitrary variable chosen will be a special uniform or Gaussian variable. For that reason, $J(.)$represents the generator function and $R(.)$represents discriminator function. Nevertheless, eq. (14) represents the value function $T(J,R)$ wherein, $R(X)$represents the sigmoid function which is used to model probability outcome to identify the accurate image by means of the discriminator, as well as $J(k)$indicates synthetic information on basis of the distribution. Moreover, $\beta_{t_1 \sim t_2}$ denotes random variable expectation of t_1 samples from the distribution of t_2. The discriminator is exploited to recognize if the input is a synthetic or real image. Eq. (16) states the GAN loss function wherein, d represents a number of samples. By exploiting the generator the synthetic image is produced. For that reason, the generator attempt to reduce the increase of discriminator, and this procedure is known as the loss function of generator R_{loss} that is stated as eq. (17). Therefore, the generator loss function, as well as discriminator, is trained by exploiting the adopted optimization approach.

$$T(J,R) = \beta_{X \sim Y_{data}} [\log R(X)] + \beta_{X \sim J_{dis}} [\log(1 - R(X))] \tag{14}$$

$$T(J,R) = \beta_{X \sim Y_{data}} [\log R(X)] + \beta_{X \sim K} [\log(1 - R(J(k)))] \tag{15}$$

$$R_{loss} = -\frac{1}{d} \sum_{c=1}^{d} V_c \log(R(X_c)) - \frac{1}{d} \sum_{c=1}^{d} (1 - V_c) \log(1 - R(X_c)) \tag{16}$$

$$J_{loss} = \max_{R} . T(R,J) \tag{17}$$

3.5.2 Training Procedure of GAN by Exploiting Adopted FPO-BPSO Approach

The GAN training procedure is performed by exploiting the proposed Hybrid FPO and BPSO that are modeled by combining FPO and BPSO, respectively.

In this work, a Hybrid Flower Pollination algorithm with the Binary Particle Swarm Optimization algorithm [12] based GAN (FPO-BPSO based GAN) is proposed, for the detection of Osteosarcoma.

Nevertheless, using the S-shaped transfer function the search space is frame-and worked in the adopted model also uses the new switch probabilities. As a solution binary vector is used, subsequently 1 equivalent if a feature will be chosen to create a new dataset as well as zero otherwise. In FPA as well as PSO, Eq. (18) is used just to create novel solutions to binary values.

The formulation of the binary vector is represented as below:

$$S\left(x_i^j(t)\right) = \frac{1}{1 + e^{V_i^j(t)/2}} \tag{18}$$

$$S\left(x_i^j(t)\right) = \frac{1}{1 + e^{x_i^j(t)}} \tag{19}$$

$$x_i^{'j}(t) = \begin{cases} 1 \text{ if } S\left(x_i^{'j}(t)\right) > \sigma \\ 0, \text{ other wise} \end{cases} \tag{20}$$

wherein σ indicates a uniform distribution count in [0, 1]. Hence, solutions keep unaltered in their locations while values of their step size increase. In addition, a new process has been augmented in the local pollination step on the basis of the optimal solution until now for intensification as below:

$$x_i^{'j}(t) = \begin{cases} g^{*j} \text{ if rand} > \beta \\ x_i^{'j}(t), \text{ other wise} \end{cases} \tag{21}$$

wherein rand indicates a uniform distribution count in [0, 1]. This process is to improve searchability to obtain the best solution with the option to find the optimum solution in shows potential area. Subsequently, using the V-shaped transfer function the search space is designed and exploits the similar new switch probabilities in the proposed model. The V-shaped is used to attain- the step size attains from the proposed model as Eq. (23). On basis of the proposed model laws, the location of a given solution is updated, when maintaining the binary limitation on basis of the present solution.

$$H_i^j(t) = \left| \frac{2}{\Pi} \arctan\left(\frac{\pi}{2} \times S_i^j(t) \right) + 0.05 \right| \quad (22)$$

$$x_i^j(t+1) = \begin{cases} 1 - x_c^j(t), \text{ if } H_i^j(t) > \sigma \\ x_i^j(t), \text{ otherwise} \end{cases} \quad (23)$$

wherein $x_c^j(t)$ indicates an arbitrary solution chosen from the current population and σ indicates a uniform distribution number in [0, 1]. On the basis of eq. (17), the parameter β is updated linearly in each iteration within the range from 0.9 to 0.2.

$$\beta = 0.9 - \frac{0.7t}{T} \quad (24)$$

Wherein T indicates the total number of iterations permitted for the optimization t indicates the current iteration number.

4. Result and Discussion

The experimentation analysis of adopted FPO-BPSO-based GAN for osteosarcoma detection was described in this section in this section. Moreover, the annotation was performed by two medical experts. Every image comprises a single annotation so that any image was interpreted by a single pathologist. Here, the dataset comprises 1144 images with size 1024 X 1024 at 10X resolution on the below distribution: 536 (47%) non-tumor images, 345 (30%) viable tumor tiles and 263 (23%) necrotic tumor images" [15].

This section demonstrates the analysis of FPO-BPSO-based GAN by deviating training data and K-fold. Here, the proposed method is compared with the conventional models such as SVM, deep learning, machine learning, and the ANN model.

Fig. 2 demonstrates the analysis of an adopted model for training percentage as well as K-fold. For k fold, sensitivity obtained from the adopted model obtains superior accuracy, sensitivity as well as specificity. It is obviously evident that the adopted model attained superior performance by deviating training percentage with values of 98% for sensitivity, accuracy, as well as specificity, correspondingly.

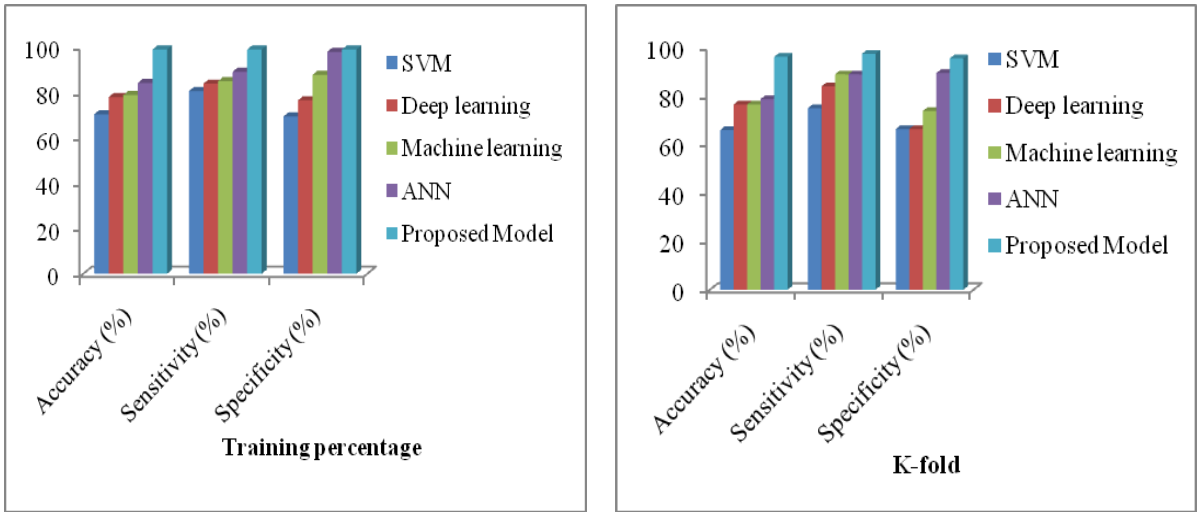

(a) (b)

Fig. 2. *Performance analysis of the proposed and conventional models (a) Training percentage (b) k-fold*

5. Conclusion

In this work, an effectual osteosarcoma recognition model was adopted by exploiting the adopted Hybrid FPO-BPSO approach. The developed technique carries out the recognition procedure by including the stages, such as pre-processing, segmentation of cells, feature extraction, and detection of osteosarcoma. At first, in pre-processing phase, the input H&E stained histology image was transmitted, wherein noise, as well as external artifacts, was evaded from the input image. Nevertheless, the pre-processed image was subjected to the cell segmentation phase; by exploiting Renyi entropy-based hybrid fusion approach cell segmentation process was performed. By combining the active contour model with blackhole fuzzy clustering, a hybrid fusion technique was modeled. After the image was segmented subsequently the

features, such as statistical, segment level as well as image-level features related to the image were efficiently extracted. Subsequent to the features extraction, the detection process was performed by exploiting the adopted Hybrid FPO-BPSO-based GAN. Finally, the adopted model attained superior performance by exploiting the measures, such as accuracy, sensitivity, and specificity.

Compliance with Ethical Standards

Conflicts of interest: Authors declared that they have no conflict of interest.

Human participants: The conducted research follows the ethical standards and the authors ensured that they have not conducted any studies with human participants or animals.

Reference

[1] Hao-Hua DengQi DengWei Chen,"Fluorescent gold nanocluster-based sensor for detection of alkaline phosphatase in human osteosarcoma cells", Spectrochimica Acta Part A: Molecular and Biomolecular Spectroscopy, 30 November 2019.

[2] Zhao-Yang WuJin-Yuan ChenAi-Lin Liu,"Sensitive electrochemical cytosensor for highly specific detection of osteosarcoma 143B cells based on graphene-3D gold nanocomposites", Journal of Electroanalytical Chemistry, 23 July 2018.

[3] F. LamonacaM. VasileA. Nastro," Measurement method for the objective and early detection of the osteosarcoma tumors", Measurement, October 2016.

[4] Ji YueZhen LiuTingbao Zhao," Bull serum albumin coated Au@Agnanorods as SERS probes for ultrasensitive osteosarcoma cell detection", Talanta1, April 2016.

[5] Lavinia Ferrante di RuffanoTony Waldron,"On the importance of considering disease subtypes: Earliest detection of a parosteal osteosarcoma? Differential diagnosis of an osteosarcoma in an Anglo–Saxon female" International Journal of Paleopathology30 December 2016.

[6] Dataset: The Cancer Imaging Archive (TCIA) Public Access: Osteosarcoma data from UT Southwestern/UT Dallas for Viable and Necrotic Tumor Assessment

[7] “https://wiki.cancerimagingarchive.net/pages/viewpage.action?pageId=52756935#bcab02c187174a288dbcbf95d26179e8”, accessed on April 2020.

[8] Liu, Jiefang, Fu-Lai Chung, and Shitong Wang, "Black hole entropic fuzzy clustering”, IEEE Transactions On Systems, Man, And Cybernetics: Systems, vol. 48, no.9, pp.1622-1636, 2017.

[9] Zheng, Youzhi, Zheng Qin, Liping Shao, and Xiaodong Hou, "A novel objective image quality metric for image fusion based on Renyi entropy”, Inf. Technol, Vol.J 7, No.6, pp.930-935, 2008.

[10] Tan Feigang, "SLBP: an improved texture feature for pedestrian detection", In proceedings of International Conference on Smart City and Systems Engineering (ICSCSE), IEEE, pp. 202-204, November 2017.

[11] Pascual, S., Bonafonte, A. and Serra, J., “SEGAN: Speech enhancement generative adversarial network”, arXiv preprint arXiv:1703.09452, 2017.

[12] Gao, Y., Kong, B. and Mosalam, K.M., “Deep leaf-bootstrapping generative adversarial network for structural image data augmentation”, Computer-Aided Civil and Infrastructure Engineering, vol. 34, no. 9, pp.755-773, 2019.

[13] Tawhid M.A., Ibrahim A.M, "Hybrid Binary Particle Swarm Optimization and Flower Pollination Algorithm Based on Rough Set Approach for Feature Selection Problem”, In: Yang XS., He XS. (eds) Nature-Inspired Computation in Data Mining and Machine Learning. Studies in Computational Intelligence, vol. 855. Springer, Cham, 2020.

[14] Neenavath Veeraiah and Dr.B.T.Krishna,"Intrusion Detection Based on Piecewise Fuzzy C-Means Clustering and Fuzzy Naive Bayes Rule", Multimedia Research, vol. 1, no. 1, October 2018.

[15] Chithra R S,Jagatheeswari P, "Enhanced WOA and Modular Neural Network for Severity Analysis of Tuberculosis", Multimedia Research, vol. 2, no. 3, July 2019.

[16] Syed Jahangir Badashah, Shaik Shafiulla Basha, Shaik Rafi Ahamed, S. P. V. Subba Rao,"Fractional-Harris hawks optimization-based generative adversarial network for osteosarcoma detection using Renyi entropy-hybrid fusion", vol.36, no. 10, pp. 6007-6031, October 2021